Virchows Arch (1999) 435:509–519 

ORIGINAL ARTICLE

**Daniele Bani · Domenico Flagiello**
**Marie-France Poupon · Silvia Nistri**
**Florance Poirson-Bichat · Mario Bigazzi**
**Tatiana Bani Sacchi**

# Relaxin promotes differentiation of human breast cancer cells MCF-7 transplanted into nude mice

Received: 3 March 1999 / Accepted: 28 May 1999

**Abstract** Previous studies showed that the hormone relaxin acts on human breast cancer MCF-7 cells in vitro by modulating cell proliferation and promoting cell differentiation toward a duct epithelial phenotype. The present study was designed to investigate whether relaxin retains these properties when acting in vivo on MCF-7 cell tumors developed in athymic nude mice. Mice bearing MCF-7 cell tumors transplanted under the mammary fat pad and estrogenized to sustain tumor growth were treated systemically with relaxin (10 µg/day) for 19 days. Vehicle-treated mice were used as controls. Thirty days later, the mice were sacrificed and tumor fragments were analyzed by light and electron microscopy and immunocytochemistry. Measurements of tumor volume were recorded weekly for the overall experimental period. The results obtained indicate that relaxin treatment promotes differentiation of tumor cells towards both myoepithelial-like and epithelial-like cells, as judged by the ultrastructural features of the cells and by the increased expression of smooth muscle actin and cadherins. Measurements of tumor size and of the number of cycling cells show that relaxin, at the doses and times of exposure used in this study, does not significantly influence tumor growth and cell proliferation.

**Key words** Relaxin · Breast cancer · MCF-7 cells · Nude mice

D. Bani · S. Nistri · T. Bani Sacchi (✉)
Department of Anatomy, Histology and Forensic Medicine, Section of Histology, University of Florence, V.le Pieraccini 6, I-50139 Florence, Italy
e-mail: histology@cesit1.unifi.it
Tel.: +39-55-4271390, Fax: +39-55-4271385

D. Flagiello · M.-F. Poupon · F. Poirson-Bichat
Institut Curie, Paris Cedex 05, France

M. Bigazzi
Prosperius Institute, Florence, Italy

## Introduction

The peptide hormone relaxin (RLX) has been found to have a marked mammotrophic action, being able to stimulate growth of the mammary gland and to promote differentiation of ductal blasts into both epithelial and myoepithelial cells (reviewed in [2, 5]). Previous studies from our group have also shown that RLX influences the behavior of human breast cancer cells cultured in vitro [6–9]. In these studies we used the breast adenocarcinoma MCF-7 cell line because of its responsiveness to mammotrophic hormones [13]. RLX has been found to have a biphasic action on MCF-7 cells, stimulating their proliferation at low, nanomolar concentrations and inhibiting it at high, micromolar concentrations [9]. When applied to MCF-7 cells for prolonged exposure times, RLX has been shown to inhibit cell proliferation at any concentration assayed and to promote cell differentiation in terms of polarization of organelles and expression of cell–cell adhesion molecules, thus leading MCF-7 cells to acquire a phenotype reminiscent that of epithelial cells of normal mammary ducts [6, 8].

The above in vitro studies suggest that RLX can be included among the hormones capable of influencing growth and differentiation of human breast cancer. However, the clinical significance of the in vitro observations is difficult to interpret owing to the lack of host-related factors that may affect tumor behavior in vivo. The present study was designed to investigate whether RLX retains the properties observed in MCF-7 cell cultures when acting in vivo on MCF-7 cell tumors grown in athymic nude mice.

## Materials and methods

### Animals

The animals used were congenitally athymic homozygous nude mice on a Swiss background, bred and maintained at the Institut Curie, Paris, France. The mice were sexually mature females, 6 weeks old. They were housed in specific pathogen-free conditions

under a 12-h light–dark photoperiodicity and with humidity and temperature controlled. Boxes, bedding, food and water were sterilized. Sterility was maintained during the surgical procedures used for the inoculation of MCF-7 cells to give rise to solid tumors and for subsequent removal and transplantation of MCF-7 cell tumors as described below. Surgery was carried out during a brief ethyl ether anesthesia. At the end of the experiments, the mice were sacrificed by neck elongation. The experimental protocol was designed in compliance with the *Principles of Laboratory Animal Care* (NIH publication no. 85-23, revised 1985) and the recommendations of the European Economic Community (86/609/CEE) and of the French Ministère de l'Agriculture, and under the supervision of a competent local committee on the care and use of laboratory animals.

## Culture of MCF-7 cells and induction of tumors

MCF-7 cells were grown in DMEM with 10% fetal calf serum (Gibco, Grand Island, N.Y., USA). Cultured cells were harvested at log phase growth, adjusted to a concentration of $10^7$ cells/0.3 ml DMEM, placed on ice until needed and finally inoculated under the mammary fat pad of nude mice through a 22-G needle tunneled 1–2 cm to prevent leakage of the inoculum. One week before MCF-7 cell inoculation, mice each received 5 µg of 17-β estradiol valerate (Schering, Berlin, Germany), dissolved in 0.5 ml of sesame oil as repository vehicle, by s.c. injection. Estrogen injections were repeated every week to sustain tumor growth [11, 12, 16]. When solid tumors reached 8–12 mm in diameter they were surgically removed, placed in a petri dish containing fetal calf serum-free medium and dissected so that necrotic areas, which are frequently present in the central part of tumors, could be discarded. Tumor fragments of 40 $mm^3$, taken from the outer portion of the tumors, were transplanted to under the mammary fat pad of 10 nude mice.

Tumor size was evaluated by measuring two perpendicular diameters with a graduated caliper. Measurements were recorded weekly for the entire duration of the experiments. Tumor volume (V) was calculated as described previously [17] using the formula $V=a^2\times b/2$, where $a$ is the width of the tumor and $b$ is the length of the tumor, expressed in millimeters. Relative tumor volume, calculated as the ratio between the tumor volume at any given time and the volume of the same tumor at day 1, was assumed as growth index.

## Hormonal treatment of mice bearing transplanted tumors

By day 26 after transplantation, all the tumors were about the same size. At that time, the mice received s.c. injections of 17-β estradiol valerate (5 µg in 0.5 ml of sesame oil) to sustain tumor growth. Estrogen treatment was repeated weekly until sacrifice. After estrogen injections, the animals were randomly distributed into two groups of 5 mice each. The mice in the first group were treated with daily injections of highly purified porcine RLX (2500–3000 U/mg) prepared according to Sherwood and O'Byrne [19], at a dose of 10 µg/day for 19 consecutive days (from day 26 to day 45). This dose of RLX is 10-fold that found to have a clear-cut influence on the normal mammary gland in mice [3, 4]. Hence, it was expected that it would also exert an effect on the MCF-7 breast cancer cells transplanted in vivo. RLX was kindly provided by Dr O.D. Sherwood, University of Illinois, Urbana, Ill., USA. The hormone was dissolved in 0.5 ml of benzopurpurine 1% in PBS as repository vehicle, which allows a slow release of the hormone over 24 h. The mice in the second group were treated with daily injections of vehicle alone and were used as controls. Both RLX and vehicle were withdrawn at day 45, and tumor growth was monitored for a further 30 days. Owing to marked slowness of the growth of MCF-7 cell tumors in vivo, we chose to wait 30 days after RLX withdrawal, to afford this hormone enough time to show its putative effects on tumor growth. With the above regimen we also aimed at recreating the physiological condition, in which RLX is not continuously present in blood, being detectable only during the luteal phase of the menstrual cycle [10, 21]. At day 76, the mice in both groups were sacrificed and their tumors were excised and processed for morphologic analysis, as described below.

To verify that RLX had reached circulating levels capable of evoking specific biologic responses, we paid attention to the mammary glands, which are typical targets for RLX [5]. As expected, RLX administration to nude mice caused a marked elongation of the nipples and growth of the mammary glands, judging by the greater increase in size of these organs recognizable on visual examination as compared with the mice not treated with RLX. Moreover, in the RLX-treated mice, histological examination of the mammary tissue near the excised tumors showed branched mammary ducts with numerous cells immunoreactive for proliferating cell nuclear antigen (PCNA), which identifies cycling cells [22]. These findings can be considered as the expression of growing mammary gland parenchyma.

## Morphology

Each tumor was divided into two moieties, one of which was processed for light microscopy and immunocytochemistry and the other one cut in small fragments which were processed for electron microscopy.

For light microscopy, the tumor tissue was fixed by immersion in isotonic 4% paraformaldehyde in phosphate-buffered saline (PBS), pH 7.4, dehydrated in graded ethanol, and embedded in paraffin wax. Sections 5 µm thick were cut and stained with hematoxylin and eosin. Light microscopic examination was also carried out on semithin sections, 2 µm thick, obtained from specimens processed for electron microscopy and stained with toluidine blue–sodium tetraborate.

For electron microscopy, small tissue fragments were fixed in cold 4% glutaraldehyde in 0.1 M sodium cacodylate buffer, pH 7.4, for 3 h at room temperature, and postfixed in 1% osmium tetroxide in 0.1 M phosphate buffer, pH 7.4, for 1 h at 4°C. They were then dehydrated in graded acetone, passed through propylene oxide and embedded in Epon 812 (Fluka, Buchs, Switzerland). Ultrathin sections were stained with uranyl acetate and alkaline bismuth subnitrate and viewed under a JEM 1010 electron microscope (Jeol, Tokyo, Japan) at 80 kV.

For immunocytochemistry, sections 5 µm thick were cut from the paraformaldehyde-fixed, paraffin-embedded specimens. The sections were subjected to immunostaining with the following antisera:

- Mouse monoclonal anti-PCNA (Labometrics, Milan, Italy; working dilution 1:30) to evaluate the number of cycling cells [22]. As positive controls, cultures of MCF-7 cells at log-phase of growth were used.
- Mouse monoclonal anti-α smooth muscle actin (Sigma, St Louis, Mo., USA; working dilution 1:300), which is a marker of differentiation for myoepithelial cells. As positive controls, sections of normal human salivary glands, which contain numerous myoepithelial cells, were immunostained together with the sections from the MCF-7 cell tumors.
- Rabbit polyclonal anti-pan-cadherin (Sigma; working dilution 1:800) to identify intercellular junctions, which are regarded as a reliable marker of epithelial differentiation of breast cancer cells [8, 20]. As positive controls, sections of normal human epidermis were immunostained together with sections from the MCF-7 cell tumors. Sections were treated with 0.05% trypsin in PBS, pH 7.4, for 10 min at room temperature before immunostaining to improve binding of antibodies to their specific antigens.

The antisera used were chosen for their ability to react with human antigens. They were diluted in Tris-buffered saline (TBS) and applied to sections overnight at 4°C. Immune reaction was revealed by biotinylated goat anti-mouse or anti-rabbit immunoglobulins, followed by streptavidin-conjugated alkaline phosphatase. Enzyme activity was revealed by incubation with naphthol As-Bi

phosphate (Sigma) as substrate and with New Fuchsin (Sigma) as chromogen. Negative controls were carried out by substituting the primary antisera with nonimmune sera. When needed, sections were counterstained with Mayer's hemalum. Counterstaining was not carried out in the sections used for computer-assisted morphometry, as described below.

### Quantitative evaluation of proliferating cells

To this aim, sections immunostained to reveal PCNA were used. From each tumor, three microscopical fields at ×540 magnification were chosen at random from three different areas of tumor tissue. In each field, the numbers of positive and negative cells were recorded and the percentage of positive cells was calculated. Two different observers, unaware of whether the sections came from RLX-treated or control mice, evaluated the same microscopical fields and individual values were then averaged.

### Computer-assisted morphometry

This was carried out to evaluate: (i) the tissue area immunolabeled for α-smooth muscle actin, which is related to the presence of cells showing a myoepithelial phenotype; (ii) the tissue area immunolabeled for pan-cadherin, which is related to the presence of cells able to form intercellular junctions. Measurements were performed according to the method described previously for similar purposes [14]. From each tumor, 5 microscopical fields at ×1,240 magnification were chosen at random from different areas of tumor tissue. Therefore, in the control and the RLX-treated groups, 25 microscopical fields, 5 from each animal in the groups, were analyzed. The fields were viewed by a CCTV television camera (Sony, Tokyo, Japan) applied to a light microscope and interfaced with an Apple Macintosh LC III personal computer through a Videospigot card (Supermac, Sunnyvale, Calif., USA). The card allows for the light transmitted across the microscopical slide to be determined within a range of 256 gray levels, which range between 0 (black level) and 255 (white level). The card also allows for digitized images of the microscopical fields to be reproduced on the basis of the values estimated. Threshold values of light transmission characteristics of the immune reactions were determined and the corresponding tissue areas were measured using the free-share Image Analysis Program, version 1.49 (National Institute of Health, Bethesda, Md., USA).

### Statistical analysis

The data reported are expressed as means ± SEM. Statistic analysis was performed by Student's *t* test for unpaired values. Calculations were carried out using a GraphPad Prism 2.0 statistical program (GraphPad Software, San Diego, Calif., USA). $P<0.05$ was considered significant.

## Results

### Architectural pattern of MCF-7 cell tumors

The MCF-7 cell tumors transplanted to the mammary region of nude mice appeared as round or ovoid masses encapsulated by a thin, discontinuous connective tissue capsule. All the tumors had similar microscopic organization (Fig. 1). Neoplastic MCF-7 cells were clustered at the periphery, forming an epithelial-like cortex that was thicker on the side facing the mammary gland and thinner on the opposite side. The central core of the tumor was made up of fibrous connective tissue. Sprouts of neoplastic cells continuous with the inner aspect of the epithelial-like cortex could often be seen penetrating the central core, in which necrotic areas could sometimes be observed. The tumors were virtually devoid of blood vessels. On the other hand, numerous microvessels were seen within the capsule and in the mammary fat pad adjacent to the tumor.

**Fig. 1** Low-power view of a MCF-7 cell tumor developed in a nude mouse. Epithelial-like cortex is thick on the side facing the mammary gland and thin on the opposite side. The central core of the tumor is made up of fibrous connective tissue. Sprouts of neoplastic cells penetrating the central core and a necrotic area (*arrow*) can be seen. Hematoxylin and eosin, ×9, *bar* 1 mm

No appreciable differences were seen in the architechtural pattern and vascularity between the tumors grown in control mice and those grown in the RLX-treated mice.

### Growth pattern of MCF-7 cell tumors

Measurement of tumor volume showed that the tumors grew slowly before the onset of hormonal treatments and that tumor growth increased progressively after the administration of estrogen. RLX treatment had little real effect on tumor growth, since the mean volume of the tumors from the RLX-treated mice, although slightly greater, was not significantly different from that of the tumors from the control mice, either at the end of the RLX treatment (day 45: control: 3.2±0.6, RLX-treated: 5±1.1) or at the end of the experimental period (day 76: control: 7.3±1.3; RLX-treated: 11.9±3.3).

Owing to the peculiar architecture of the MCF-7 cell tumors grown in nude mice, measurements of total tumor size

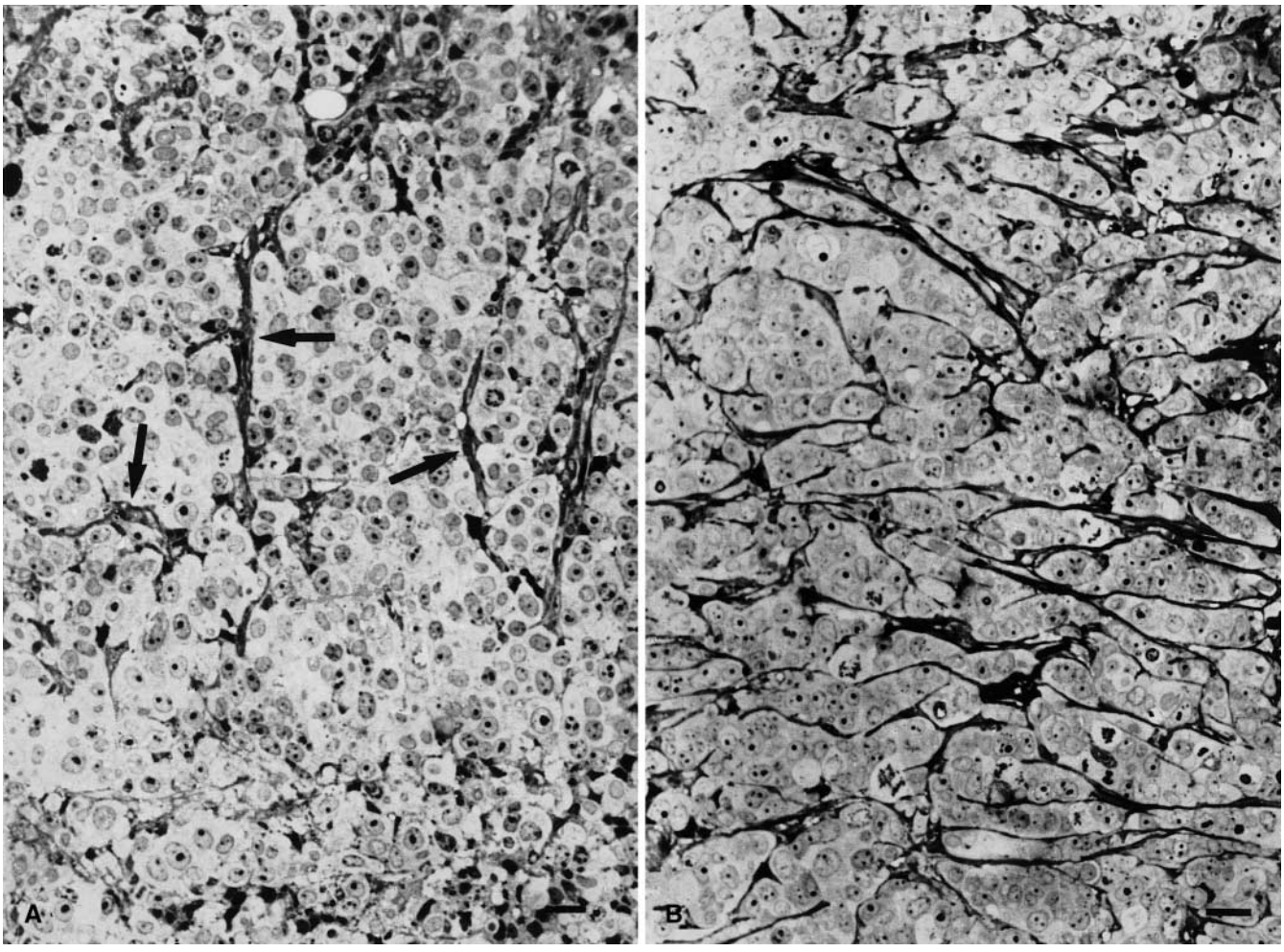


**Fig. 2A, B** Histological appearance of the epithelial-like cortex of MCF-7 cell tumors. **A** Control mice: polyhedral cells are arranged in large clusters; a few stellate cells with long cytoplasmic processes can be seen (*arrows*). **B** RLX-treated mice: polyhedral cells form small clusters; stellate cells are very numerous. Semithin section stained with toluidine blue-sodium tetraborate, ×260, *bar* 20 μm

do not provide adequate information as to the real growth of tumor tissue. In fact, the neoplastic cells are confined to the epithelial-like cortex, whereas the inner core probably corresponds to a desmoid reaction of the host to the tumor implant. Therefore, to achieve more precise information on the effect of RLX on neoplastic cell growth, we evaluated the amounts of cycling cells in the epithelial-like cortex. The results of PCNA immunocytochemistry showed that the percentage of cycling cells in the RLX-treated mice, although slightly lower, was not significantly different than in the controls (control: 29.4±6.2; RLX-treated: 25.5±4.8).

## Light and electron microscopy of MCF-7 cell tumors

### *Tumors from control mice*

The epithelial-like cortex of the tumors was composed of cells arranged in solid masses with almost no intervening connective tissue septa. These cells were mostly polyhedral in shape, with a high nuclear-cytoplasmic ratio, nuclei with dispersed chromatin and prominent nucleoli, and slightly basophilic cytoplasms. Mitoses were rather frequently seen. A minority of the tumor cells were stellate, with long cytoplasmic processes and nuclei with coarse chromatin clumps (Fig. 2A). These latter cells were usually dispersed between the polyhedral ones and sometimes grouped together in large clusters.

By electron microscopy, the polyhedral cells had an undifferentiated phenotype (Fig. 3A), with cytoplasm containing many free polyribosomes, a few mitochondria and cisternae of rough endoplasmic reticulum, and a

**Fig. 3A–D** Ultrastructural appearance of the epithelial-like cortex of MCF-7 cell tumors from control mice. **A** Polyhedral cells show nuclei with dispersed chromatin and large nucleoli and cytoplasms rich in free polyribosomes. ×4,000, *bar* 2 μm **B** Rudimentary desmosomes between two polyhedral cells (*arrows*). ×40,000, *bar* 0.5 μm **C** Detail of the cytoplasm of stellate cells showing numerous cisternae of rough endoplasmic reticulum, bundles of myofilaments with interspersed dense bodies (*arrows*), and a discontinuous basal lamina (*arrowheads*). ×30,000, *bar* 0.5 μm. **D** Degenerating cells, with coarse chromatin clumps and cytoplasm lysis, at the transitional area between the epithelial-like cortex and the inner connective tissue core. ×6,000, *bar* 2 μm

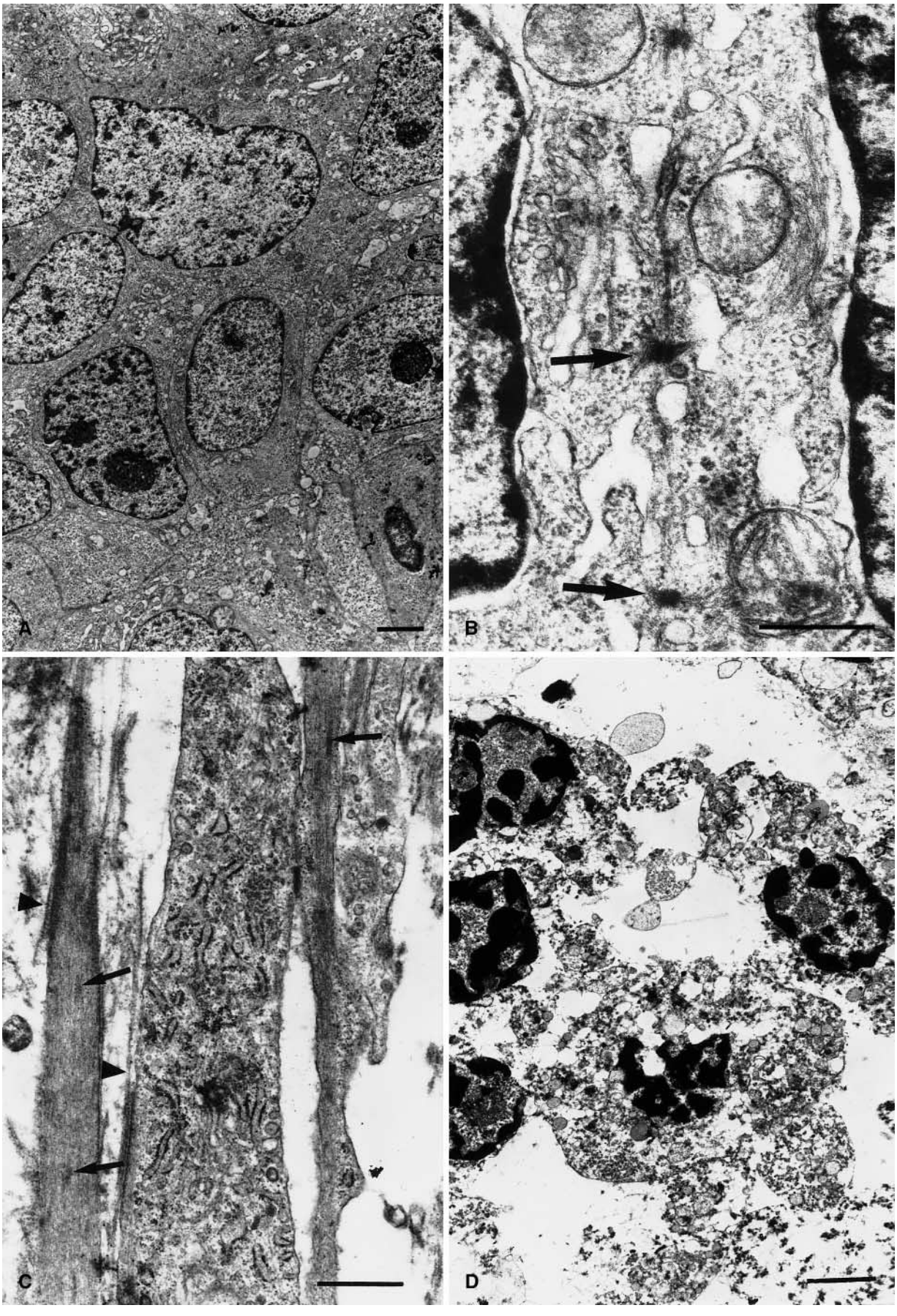
A
B
C
D

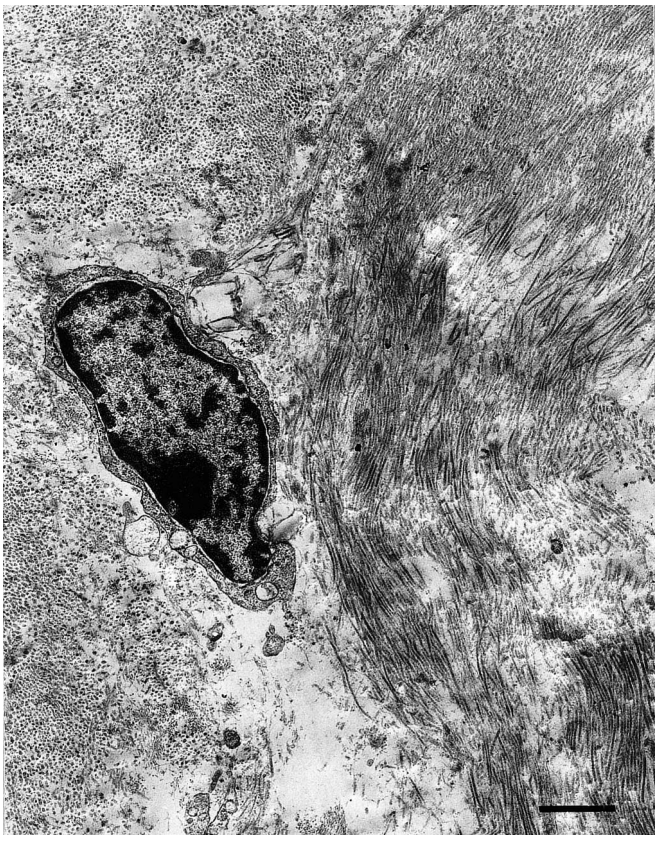

**Fig. 4** Ultrastructural appearance of the connective tissue core of MCF-7 cell tumors from control mice. A fibroblast is seen surrounded by coarse bundles of collagen fibers. ×10,000, *bar* 1 µm

**Fig. 5** Ultrastructural appearance of the epithelial-like cortex of a MCF-7 cell tumor from a RLX-treated mouse. Small clusters of polyhedral cells are separated by stellate cells, recognizable for condensed chromatin and electron-dense cytoplasmic matrix. ×4,000, *bar* 2 µm

small Golgi apparatus. Intercellular junctions were an occasional finding and consisted mainly of rudimentary desmosomes (Fig. 3B). Compared with the polyhedral cells, the stellate cells had denser cytoplasmic matrix, more developed rough endoplasmic reticulum and larger Golgi apparatus. They were characterized by the presence of bundles of myofilaments, often with interspersed dense bodies, mainly located at the periphery of the cell body and within the cytoplasmic processes. Microvesicles opened at the cell surface could also be seen, as could a discontinuous basal lamina over the plasma membrane (Fig. 3C). These cells feature early differentiating myoepithelial cells.

Several degenerating cells, with coarse chromatin clumps and cytoplasm lysis, were concentrated in the transitional area between the epithelial-like cortex and the inner connective tissue core (Fig. 3D).

The connective tissue core contained sparse fibroblasts and coarse collagen bundles (Fig. 4).

*Tumors from RLX-treated mice*

Clear-cut differences could be observed in the tumor cells of the epithelial-like cortex compared with the tumors from the control mice. By light microscopy, in the RLX-treated mice stellate cells were far more numerous than in the controls. In some areas, these cells formed an extended network embedding rather small clusters of polyhedral cells (Fig. 2B). By electron microscopy, stellate cells were in close contact with polyhedral cells (Fig. 5) and showed the features of myoepithelial cells at varying degrees of differentiation. Some of them resembled poorly differentiated myoepithelial cells (Fig. 6A),

**Fig. 6A, B** Ultrastructural appearance of the epithelial-like cortex of MCF-7 cell tumors from RLX-treated mice. **A** A stellate cell featuring an early developing myoepithelial-like cell: note the presence of scattered bundles of myofilaments (*arrows*) and dense plaques adherent to the plasma membrane (*arrowheads*). ×20,000 **B** Cytoplasmic processes of stellate cells containing large bundles of myofilaments, dense plaques (*arrows*) and an almost continuous basal lamina (*arrowheads*). ×30,000, *bar* 0.5 µm

**Fig. 7A, B** Ultrastructural appearance of the epithelial-like cortex of MCF-7 cell tumors from RLX-treated mice. **A** Polyhedral cells showing abundant organelles, bundles of intermediate filaments and several intercellular junctions. ×20,000 **B** Two polyhedral cells are joined by well-developed desmosomes. ×40,000, *bar* 0.5 µm

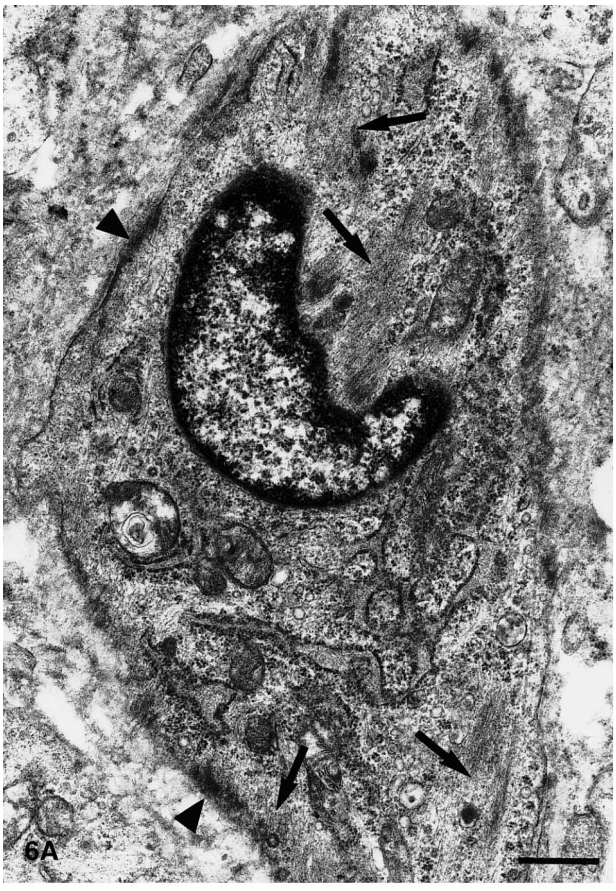
6A

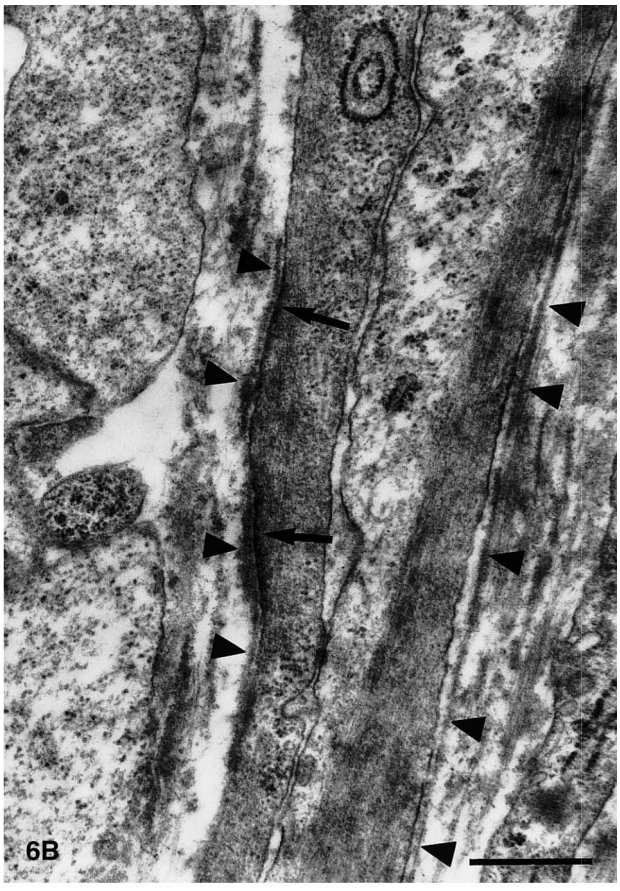
6B

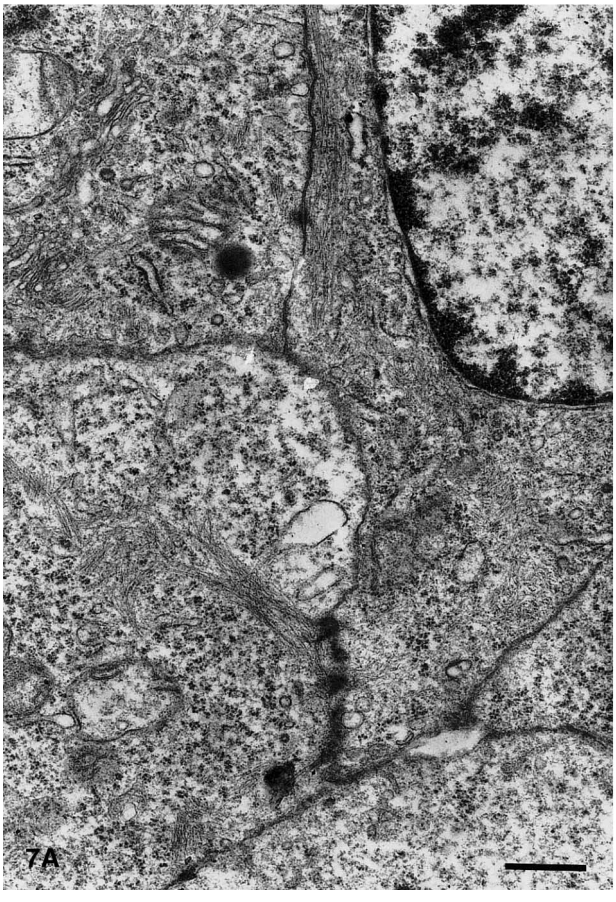
7A

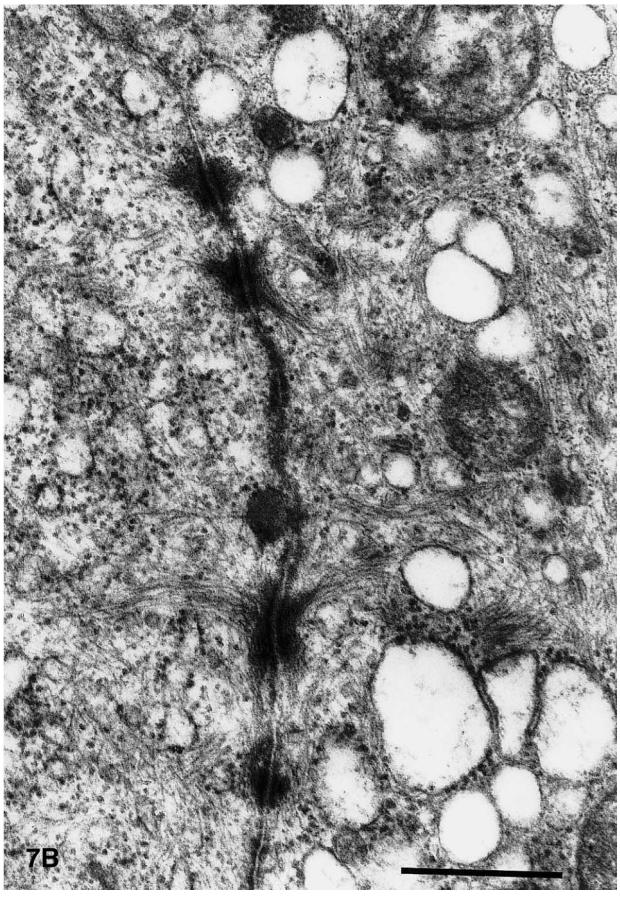
7B

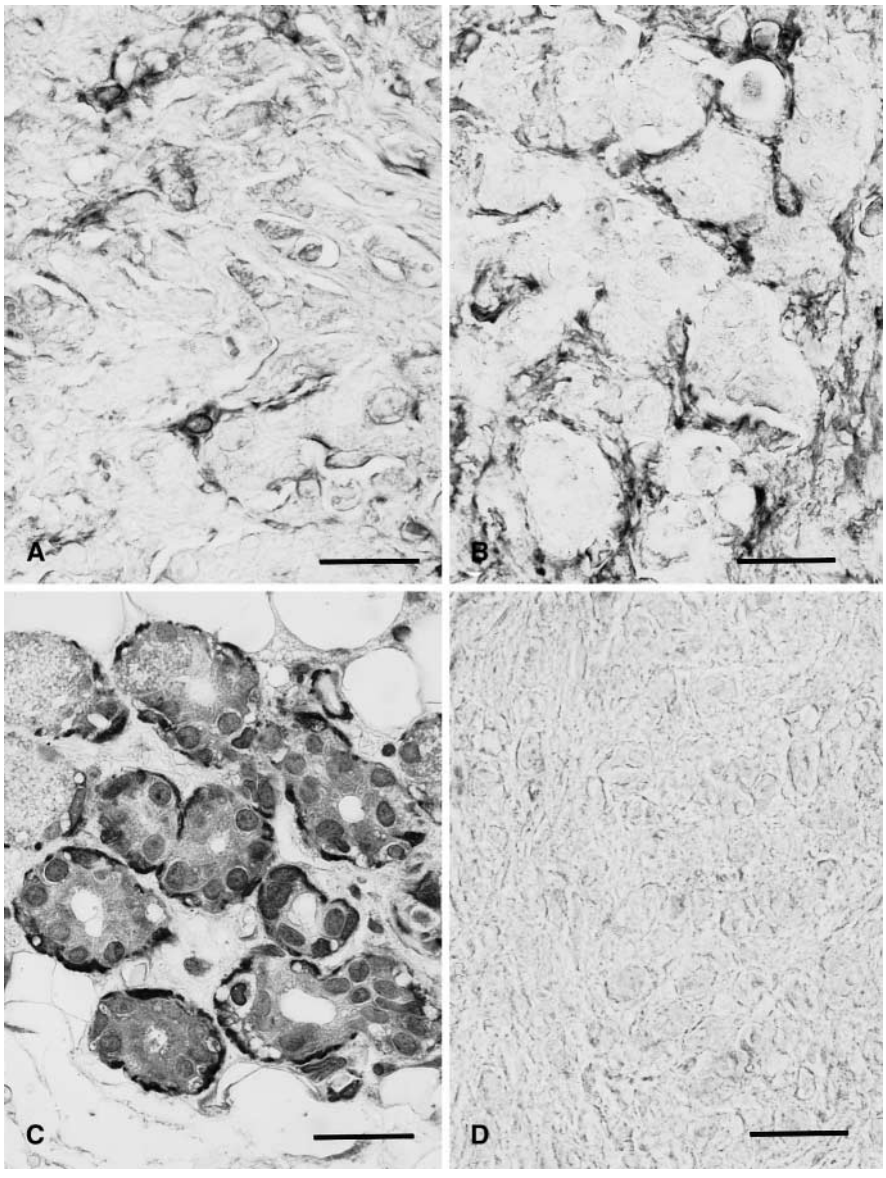


**Fig. 8A–D** Immunoreactivity for α smooth muscle actin. Epithelial-like cortex of MCF-7 cell tumors in: **A** control mice, showing a few immunostained cells with long cytoplasmic processes, and **B** RLX-treated mice, showing numerous positive cells forming a network; **C** positive control: immunostained myoepithelial cells surrounding secretory units in a normal human salivary gland; **D** negative control: epithelial-like cortex of MCF-7 cell tumor treated with nonimmune mouse serum in the place of the primary antibody. ×650, *bar* 20 μm

similar to those observed in the control tumors. Some others featured myoepithelial cells in more advanced stages of differentiation (Fig. 6B), as judged by the presence of nuclei with condensed chromatin, coarse bundles of myofilaments intermingled with dense bodies and adherent to dense plaques apposed to the plasma membrane, intercellular junctions of the adherent type, and an almost continuous basal lamina. In the intercellular spaces, strands of moderately electron-dense material similar to that of basal lamina were seen. Cytological signs of differentiation towards an epithelial phenotype could also be observed in polyhedral cells. In fact, besides undifferentiated cells, other cells were found with increased organelle complement and abundant cytoskeletal filaments (Fig. 7A). These cells were linked by well-developed desmosomes and intermediate junctions (Fig. 7B).

### Actin and pan-cadherin expression by MCF-7 cell tumors

In the epithelial-like cortex of the tumors from control and RLX-treated mice, cells immunoreactive for either α-smooth muscle actin or pan-cadherin were observed. Actin immunoreactivity was localized within the cell cytoplasm, whereas pan-cadherin immunoreactivity was localized both at the cell membrane and within the cytoplasm. A visual examination disclosed that a few cells of the tumors from control mice were immunoreactive for α-smooth muscle actin and pan-cadherin. In contrast, in the tumors from RLX-treated mice, cells immunostained for these proteins were more frequently seen (Figs. 8, 9). Computer-assisted morphometry revealed that the surface area of tissue immunostained for α-smooth muscle actin and pan-cadherin was significantly increased following RLX treatment (Fig. 10).

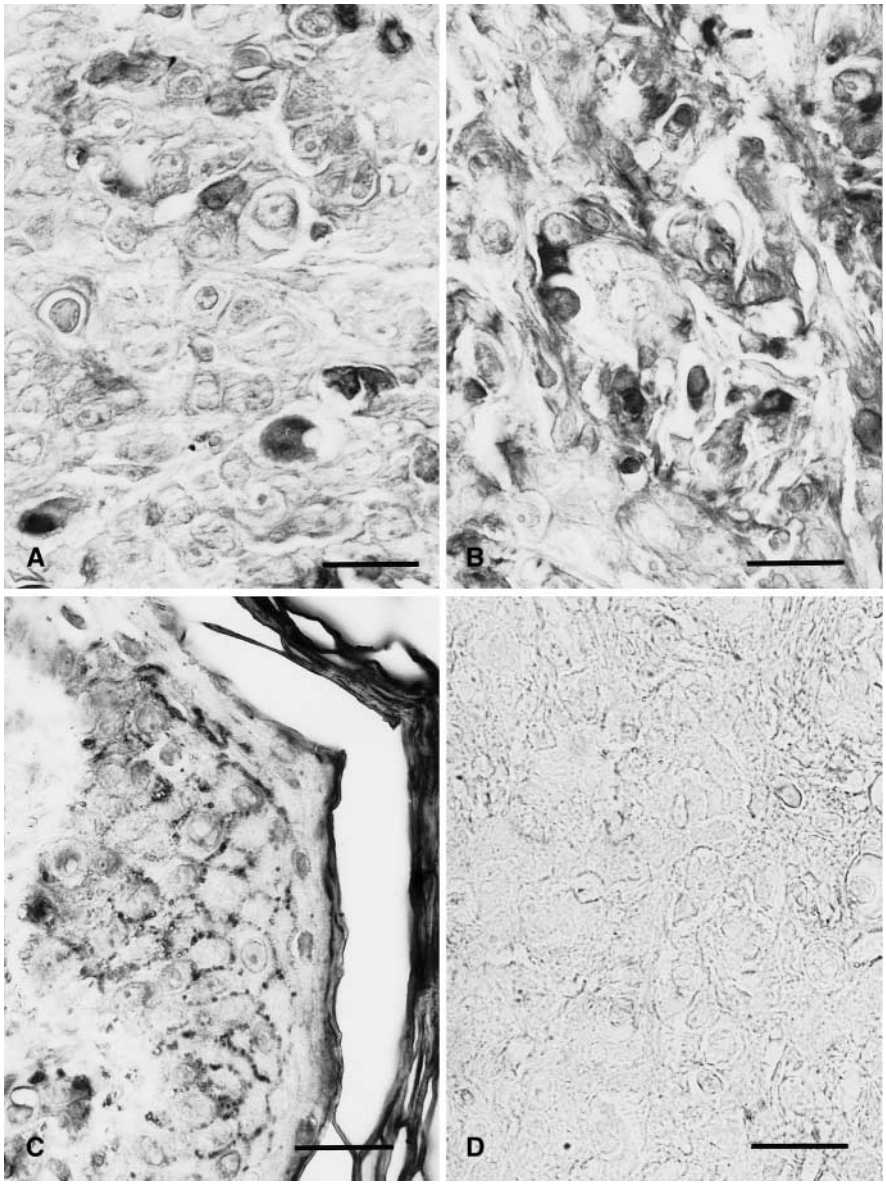


**Fig. 9A–D** Immunoreactivity for pan-cadherin. Epithelial-like cortex of MCF-7 cell tumors in: **A** control mice, showing a few immunostained cells, and **B** RLX-treated mice, showing several fairly positive cells; **C** positive control: normal human epidermis showing immunoreactive desmosomes; **D** negative control: epithelial-like cortex of MCF-7 cell tumor treated with nonimmune rabbit serum in the place of the primary antibody. ×650, *bar* 20 μm

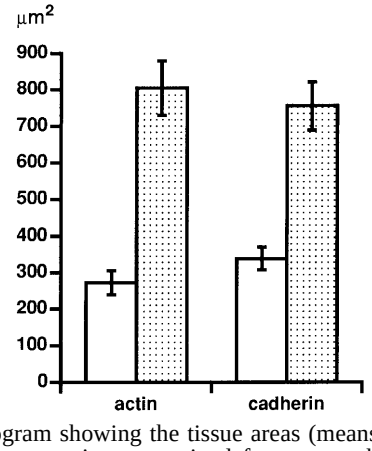


**Fig. 10** Histogram showing the tissue areas (means±SEM) of the epithelial-like cortex immunostained for α smooth muscle actin and pan-cadherin. Significance of differences between groups (each group $n$=25; Student's $t$-test) $P$<0.0001 (*open columns* control mice, *dotted columns* RLX-treated mice)

## Discussion

The results of this study show that RLX, administered systemically to estrogenized nude mice bearing heterotransplanted MCF-7 cell tumors, promotes differentiation of tumor cells towards a dual myoepithelial and epithelial phenotype. In fact, in the control tumors, most cells are polyhedral in shape and show an immature, blast-like phenotype, similar to the original characteristics of MCF-7 cells in vitro [6, 8], whereas other cells have the features of early differentiating myoepithelial cells. Upon RLX treatment, myoepithelial-like cells become more numerous and often show cytological signs of more advanced differentiation. In the meantime, several polyhedral cells are also prompted to acquire a distinct epithelial phenotype, as judged by the increase in organelles, cytoskeleton and intercellular junctions. The finding that immunostaining for pan-cadherin is local-

ized not only at the cell surface but also within the cytoplasm may be consistent with de novo synthesis of these adhesion molecules by the proteosynthetic machinery of differentiating MCF-7 cells.

The current findings are in agreement with the results of our previous studies on MCF-7 cells in vitro, in which RLX was shown to promote differentiation and to enhance cell–cell adhesion through the expression of cadherin [6, 8]. It is tempting to speculate that RLX, which is able to induce breast cancer cells to acquire a myoepithelial-like phenotype and to increase intercellular adhesion, might also hinder local invasiveness of the MCF-7 cell tumors. In this context, it should be pointed out that noninvasive intraductal carcinomas of the breast are characterized histopathologically by the presence of myoepithelial cells enveloping the tumor cell clusters, and that the cells of the invasive foci of infiltrating ductal carcinomas lack any relationships with myoepithelial cells [1].

It is widely accepted that growth and differentiation of breast cancer cells can be influenced by normal mammary gland components (reviewed in [15, 18]). The present study agrees with this assumption, since it shows that the MCF-7 tumor parenchyma was growing more actively on the side facing the mammary tissues than on the opposite side. Moreover, the cells of the transplanted tumors, grown under the influence of the adjacent mammary tissues, can attain a higher degree of differentiation than they did when growing in vitro. It is noteworthy that in nude mice, the MCF-7 cells are prompted to enter the differentiation pathway leading to both epithelial- and myoepithelial-like cells, thus giving rise to mixed tumors. This is at variance with previous studies on MCF-7 cells cultured in vitro, which showed that, in the absence of integrated host-derived stimuli, these cells could only be prompted to differentiate towards an epithelial phenotype [6, 8]. Indeed, a dual differentiation potential is known to be intrinsic to normal precursor cells located in the mammary ducts, which are responsible for the growth of mammary gland parenchyma in appropriate physiological conditions [3, 4]. On the basis of all this, MCF-7 cells may be regarded as neoplastic bipotential stem cells of ductal origin, which could progress towards an epithelial or myoepithelial phenotype if properly stimulated by local and systemic signals. Among these signals, RLX seems to have a major role.

RLX, when given according to the administration regimen investigated in this study, has a clear-cut differentiation-promoting action on the MCF-7 cells of the tumors but has no significant effect on MCF-7 cell growth, judging by the overall tumor size and the percentages of cycling cells. This is in contrast with the previously reported in vitro effects of RLX on MCF-7 cells, which can be either growth stimulated or growth inhibited, depending on the RLX concentrations and times of exposure [7–9]. Our experimental model does not allow us to establish whether RLX administered systemically to nude mice had reached the MCF-7 cells of the tumors at growth-promoting or growth-inhibiting concentrations. In any event, the reasons for the observed ineffectiveness of RLX in promotion or inhibition of growth of MCF-7 cell tumors in vivo remain unknown. It appears that the MCF-7 cells are unable to induce neovascularization of the tumor mass. This may hinder the blood supply and hence reduce cell growth to a critical level, thus blunting the effects of agents potentially able to promote cell growth, including RLX. On the other hand, even if RLX had been able to inhibit tumor cell growth, its effect might have been counterbalanced by growth-promoting stimuli, such as local mammotrophic factors, which are known to be released by the mammary tissues adjacent to the tumors [15, 18].

**Acknowledgements** The authors gratefully acknowledge Dr. O.D. Sherwood, of the Department of Molecular and Integrative Physiology, University of Illinois at Urbana Champaign, Urbana, Ill., USA, who kindly provided purified porcine relaxin as a gift. Many thanks are also due to Mr. Vincent Bodier, Institut Curie, Paris, France, to Ms. Laura Calosi and to Mr. Patrizio Guasti, Department of Anatomy, Histology and Forensic Medicine, Florence, Italy, for skillful technical assistance. This study was supported by government funds from the Italian National Research Council (CNR), Rome, Italy.

## References

1. Ahmed A (1974) The myoepithelium in human breast carcinoma. J Pathol 113:129–135
2. Bani D (1997) Relaxin: a pleiotropic hormone. Gen Pharmacol 28:13–22
3. Bani G, Bigazzi M, Bani D (1985) The effects of relaxin on the mouse mammary gland. I. The myoepithelial cells. J Endocrinol Invest 8:207–215
4. Bani G, Bigazzi M, Bani D (1986) The effects of relaxin on the mouse mammary gland. II. The epithelium. J Endocrinol Invest 9:145–152
5. Bani G, Bigazzi M, Bani Sacchi T (1991) Relaxin as a mammotrophic hormone. Life Sci Adv Exp Clin Endocrinol 10:143–150
6. Bani D, Riva A, Bigazzi M, Bani Sacchi T (1994) Differentiation of breast cancer cells in vitro is promoted by the concurrent influence of myoepithelial cells and relaxin. Br J Cancer 70:900–904
7. Bani D, Masini E, Bello, MG, Bigazzi M, Bani Sacchi T (1995) Relaxin activates the L-arginine–nitric oxide pathway in human breast cancer cells. Cancer Res 55:5272–5275
8. Bani Sacchi T, Bani D, Brandi ML, Falchetti A, Bigazzi M (1994) Relaxin influences growth, differentiation and cell-cell adhesion of human breast-cancer cells in culture. Int J Cancer 57: 129–134
9. Bigazzi M, Brandi ML, Bani G, Bani Sacchi T (1992) Relaxin influences the growth of MCF-7 breast cancer cells. Mitogenic and antimitogenic action depends on peptide concentration. Cancer 70:639–643
10. Eddie LW, Martinez F, Healy DL, Sutton B, Bell RJ, Tregear GW (1986) Relaxin in sera during the luteal phase of in vitro fertilization cycles. Br J Obstet Gynaecol 97:215–220
11. Gottardis MM, Robinson SP, Jordan VC (1988) Estradiol-stimulated growth of MCF-7 tumors implanted in athymic mice: a model to study the tumoristatic action of tamoxifen. J Steroid Biochem 30:311–314
12. Huseby RA, Maloney TM, McGrath CM (1984) Evidence for a direct growth-stimulating effect of estradiol on human MCF-7 cells in vivo. Cancer Res 44:2654–2659
13. Levenson AS, Jordan VC (1997) MCF-7: the first hormone-responsive breast cancer cell line. Cancer Res 57:3071–3078

14. Masini E, Bani D, Bigazzi M, Mannaioni PF, Bani Sacchi T (1994) Effects of relaxin on mast cells. In vitro and in vivo studies in rats and guinea pigs. J Clin Invest 94:1974–1980
15. Miller WR (1992) Interactions between malignant and non-malignant components of the breast. In: Dogliotti L, Sapino A, Bussolati G (eds) Breast cancer: biological and clinical progress. Kluwer, Boston, pp 119–136
16. Osborne CK, Hobbs K, Clark GM (1985) Effect of estrogens and antiestrogens on growth of human breast cancer cells in athymic nude mice. Cancer Res 45: 584–590
17. Poupon MF, Arvelo F, Goguel AF, Burgeois Y, Jacrot M, Hanania N, Arriagada R, Chevalier TL (1993) Response of small-cell lung cancer xenografts to chemotherapy: multidrug resistance and direct clinical correlates. J Natl Cancer Inst 85:2023–2029
18. Sakakura T (1991) New aspects of stroma-parenchyma relations in mammary gland differentiation. Int Rev Cytol 125: 165–202
19. Sherwood, OD, O'Byrne EM (1974) Purification and characterization of porcine relaxin. Arch Biochem Biophys 60:185–196
20. Sommers CL, Thompson EW, Torri GA, Kemler R, Gelmann EP, Byers SW (1991) Cell adhesion molecule uvomorulin expression in human breast cancer cell lines: relationship to morphology and invasive capacities. Cell Growth Differ 2:365–372
21. Stewart DR, Celniker AC, Taylor, CA, Cragun JR, Overstreet JW, Lasley BL (1990) Relaxin in the peri-implantation period. J Clin Endocrinol Metab 70:1771–1773
22. Waseem NH, Lane DP (1990) Monoclonal antibody analysis of the proliferating cell nuclear antigen (PCNA). Structural conservation and the detection of a nucleolar form. J Cell Sci 96: 121–129